COMPUTER AIDED CRYOSTAT DESIGN IN TWENTE: RECENT DEVELOPMENTS

H.J.M. ter Brake and J. Flokstra

University of Twente, Department of Applied Physics,
P.O.Box 217, 7500 AE Enschede, The Netherlands

Some recent developments in our Computer Aided Cryostat Design are described, the first step in this project having been reported at ICEC 11. In this paper attention is paid to a faster evaluation of the temperature profile along the cryostat neck. This is used to speed up the iteration process for evaluating the heat-flux distribution in the cryostat. Further, the implementation of multi-layer superinsulation is discussed.

INTRODUCTION

Our first step towards Computer Aided Cryostat Design (CACD) has been reported at ICEC 11 [1]. The cryostat configuration was restricted to a pot type having a cylindrical helium container and a relatively narrow neck. One or more vapour-cooled radiation shields can be placed in the vacuum space in order to reduce the thermal load to the helium bath. The evaluation of the heat fluxes in the cryostat is based on two important assumptions. Firstly, the radiation shields are isothermal and secondly the heat exchange between the helium gas and the cryostat neck is ideal. The temperatures of the radiation shields are evaluated in an iterative process.

This paper describes some recent developments in our CACD project. Firstly, the cryostat model has been changed in such a way that also tail-type cryostats can be optimized. Secondly, the iteration process has been accelerated by means of a much faster evaluation of the temperature profile along the neck of the cryostat and thirdly, the application of multi-layer superinsulation (MLI) has been implemented. The first adaption being quite straightforward, attention is only paid to the latter two developments. Further, the implementation of MLI is illustrated by some optimization cases.

TEMPERATURE PROFILE ALONG THE CRYOSTAT NECK

Consider a neck tube through which helium gas is flowing with a flow rate $\dot{m}_g$. The cold end of the tube ($T=T_c$) is at $x=0$ and the warm end ($T=T_1$) is at $x=\ell$. The temperature profile along the neck is in the case of ideal heat exchange given by:

$$\lambda'(T)dT/dx = \alpha T + c_1 \qquad ; \qquad \lambda' = \lambda_t + \lambda_g A_g/A_t \tag{1}$$

where λ_t and λ_g are the thermal conductivities of respectively neck tube and gas and A_t and A_g are the cross-sectional areas. Further in eq.(1) c_1 is an integration constant determined by the boundary conditions and $\alpha = \dot{m}_g.C_p/A_t$ with C_p the heat capacity of the gas (which is considered to be constant). The evaluation of the temperature profile along the cryostat neck was in our first CACD programs carried out by dividing the neck in a large number of small sections in which λ' was considered to be constant. For such a section from $x=x_n$ to $x=x_{n+1}$ with corresponding temperatures T_n and T_{n+1}, T_{n+1} can be expressed from eq.(1) as:

$$T_{n+1} = (T_n+c_1/\alpha)\exp[\alpha(x_{n+1}-x_n)/\lambda']-c_1/\alpha \tag{2}$$

By successively applying eq.(2) the complete temperature profile along the neck was determined.

The above method is rather time consuming and therefore an alternative approach was followed. It can be shown that eq.(1) has an exact analytic solution if λ' can be expressed as a polynomial in T. With for instance $\lambda' = a_0+b_0T+c_0T^2+d_0T^3$ eq.(1) results in:

$$\alpha x = d_0(T^3-T_0^3)/3+(c_0-d_0\theta_0)(T^2-T_0^2)/2+(b_0-c_0\theta_0+d_0\theta_0^2)(T-T_0)$$
$$+(a_0-b_0\theta_0+c_0\theta_0^2-d_0\theta_0^3)\ln[(T+\theta_0)/(T_0+\theta_0)] \qquad (3)$$

in which $\theta_0 = c_1/\alpha$. In the iteration process the temperature profile along the neck is evaluated as a test for a chosen set of shield temperatures and evaporation rate. Based on heat balances on shields and container, such a set implies a specific conductive heat flow at the shields and at the container. That means that also $\lambda'(T)dT/dx$ is known at these positions. Therefore the integration constant c_1 can directly be derived from eq.(1) and substituted in eq.(3). The profile along the neck tube can then be tested by merely checking whether $T=T_1$ gives $x=\ell$.

It is clear that the iteration process is far quicker if eq.(3) is used once instead of a number of times eq.(2). The disadvantage is that the method is less accurate due to the polynomial approximation of λ'. Simulations indicate that the temperatures and heat flows are evaluated with an error of about 10%. However, with respect to other assumptions in the CACD programs as for instance the ideal gas-neck heat exchange and the MLI-model, this accuracy is very well acceptable. Using the old method based on eq.(2) this accuracy of 10% can be realized by dividing the neck tube in about 30 to 60 sections depending on the steepness of the temperature profile. However, in view of the larger complexity of eq.(3) compared to eq.(2) the resulting calculation time reduction is roughly a factor 5 to 10. This reduction especially becomes relevant if more than one radiation shield is involved [1].

MULTI-LAYER SUPERINSULATION (MLI)

The application of MLI in cryostats should be limited to regions with temperatures above about 80 K. Below this temperature the reduction of radiative heat flow can better be established by means of highly reflective tape [2]. Therefore, the MLI heat-flow model that is implemented in our CACD programs is developed for temperatures above about 80 K.

Three heat flows are of importance in MLI, i.e. radiation, residual-gas heat conduction and solid contact heat conduction. The evaluation of the heat flow through an MLI blanket is severely obstructed by the fact that a number of parameters is unknown. The most important of these parameters are emissivity coefficients, contact areas and thermal contact resistances, the residual-gas pressure and the gas heat-flow mechanism.

Several models for evaluating the heat flow through MLI have been presented in literature [3-8]. Some of these models are based on a fundamental study of heat flow mechanisms between separate layers and evaluate the overall heat flow calculating from layer to layer [3,4,6]. It is clear that this approach is far too time consuming with respect to CACD and that a model is required for the overall heat flux. The presented overall models, however, are all empirically established and are therefore only applicable to those specific MLI configurations in which the heat flows have been measured or to very similar ones. A further disadvantage of presented models is that they are mainly developed for a large number of layers (>20) whereas a few layers can already be very effective in reducing the radiative heat flow [9].

In view of the above disadvantages we had to develop our own model. It should describe the overall heat flow through an MLI blanket also permitting a small number of layers (starting from about 5), and it has to be applicable to practical MLI configurations. Very special MLI configurations resulting in extremely low conductivities as for instance presented by Scurlock and Saull [10] are not included. An important assumption in our model is that residual-gas heat conduction is neglected, and therefore the model is only applicable in the low-pressure region. Conductive gas flow becomes the dominant heat flow when the pressure in the vacuum space rises above about 10^{-4} torr [10], the pressure inside the MLI blanket being about one order of magnitude higher [11].

Our model describes the situation depicted in Fig. 1. Between a relatively hot shield having temperature T_h and a cold shield (T_c) N layers of superinsulation are

placed with an overall thickness Δx. Three regions can be separated in this configuration with corresponding heat flows: $\dot{Q}_{vac}$, the heat flow through the vacuum space from hot surface to outer MLI layer, $\dot{Q}_{MLI}$, the heat flow through the MLI blanket from outer to inner layer, and $\dot{Q}_{10}$, the heat flow from the inner MLI layer to the cold surface. Shu et al. [9] measured that even for a small number of layers the temperature of the outer layer is almost equal to that of the hot shield. For example, with T_h = 277 K and T_c = 77 K, 5 layers gave T_N = 269 K and 10 layers gave T_N = 273 K. From this study it is clear that in our model we only have to take into account $\dot{Q}_{MLI}$ and $\dot{Q}_{10}$ with $T_N = T_h$.

The heat flow $\dot{Q}_{MLI}$ through the MLI blanket per unit of area can be written as:

$$\dot{Q}_{MLI}/A = \bar{k}.[(T_N-T_1)/\Delta x].[N/(N-1)] \qquad (4)$$

with $\bar{k}$ the mean effective thermal conductivity including radiation and conduction. Barron presented this conductivity for typical MLI as a function of the layer density d_s (=N/Δx) [11], see Fig. 2, and we describe this k as:

$$\bar{k} = (\sigma\bar{\varepsilon}/d_s).[(T_N^4-T_1^4)/(T_N-T_1)] + a.d_s^{\gamma} \qquad (5)$$

A good fit is obtained with $\bar{\varepsilon}$ = 0.0341, γ = 28/9 and a = $1.668.10^{-16}$ $Wm^{19/9}K^{-1}$. As can be seen in Fig. 2 eq.(5) also coincides to a fair extent with data presented elsewhere in literature. According to the eqs.(4) and (5) $\dot{Q}_{MLI}$ can be written as:

$$\dot{Q}_{MLI}(T_N,T_1)/A = \sigma\bar{\varepsilon}(T_N^4-T_1^4)/(N-1) + a.d_s^{\gamma+1}(T_N-T_1)/(N-1) \qquad (6)$$

The heat flow Q_{10} can again be separated into conduction and radiation as:

$$\dot{Q}_{10}(T_1,T_c)/A = k_e(T_1-T_c) + [\varepsilon_1\varepsilon_e/(\varepsilon_1+\varepsilon_e(1-\varepsilon_1))].\sigma(T_1^4-T_c^4) \qquad (7)$$

with ε_e the emissivity of the cold surface, whereas k_e and ε_1 have been matched to data presented by Shu et al. [8,9]. They installed superinsulation on a black painted copper surface and on an aluminium-taped copper surface. Results were presented concerning the heat flow and the corresponding temperature of the first layer. The obtained values are k_e = 0.0063 W/(m²K) and ε_1 = 0.01.

The heat flow through an MLI blanket can now be evaluated using eqs.(6) and (7). It is also possible to consider the cold surface as the innermost layer of the MLI blanket. In this case the heat flux can be determined from eq.(6) with $T_1=T_c$ and N-1 substituted by N. It appears that the results of the models coincide if N is larger than about 20. Therefore, the heat-flux evaluation in the CACD programs uses the model based on eqs.(6) and (7) if N<20 and uses the straightforward model based on eq.(6) if N≥20. This approach is used to evaluate the heat fluxes in the experiments of Shu et al. [8,9]. The calculated and measured heat fluxes as a function of the number of layers are given in Fig. 3a. The correspondence between calculations and measurements is reasonably well. As a further comparison of model and experiments the temperature T_1 of the first MLI layer is depicted in Fig. 3b. Although the cold surface is 77 K and T_1 varies from 200 to 120 K the deviation between calculated and measured T_1 is only about 4 K.

A final test of the model was performed on data presented by Hnilicka [12]. He tested the NRC-superinsulation in a cylindrical calorimeter with a cold surface having a diameter of 4" and a temperature of 77 K (T_h = 300 K). Data and heat-flux results of the model are given in table 1.

Table 1: Heat-flux data of ref. [12] compared with the model

ε_e	Δx	N	$(\dot{Q}/A_c)_{exp}$ W/m²	$(\dot{Q}/\bar{A})_{exp}$ W/m²	$(\dot{Q}/A)_{calc}$ W/m²
0.7	0.5"	25	0.79	0.70	0.65
0.7	3"	25	1.17	0.67	0.62
0.7	0.5"	27	0.73	0.65	0.61
0.04	0.5"	25	0.75	0.67	0.65

The heat fluxes given by Hnilicka are normalized to the area A_c of the cold surface. For a useful comparison with our model, however, the heat fluxes have been normalized to the mean area $\bar{A}$ of the cylindrical MLI blanket. According to table 1, the agreement between experiments and our model is very good.

The above described MLI-model is implemented in our CACD programs and there are two possibilities. Either the MLI configuration is fixed by input (i.e. N and Δx have given values) or it is to be optimized. The optimum MLI configuration is such that the available space between hot and cold surface is completely filled with the optimum layer density, which for large N (i.e. $N/(N-1) \approx 1$), directly results from eq (5) as:

$$(d_s)_{opt} = [\sigma\bar{\varepsilon}/(a\gamma).(T_N^4 - T_1^4)/(T_N - T_1)]^{1/(\gamma+1)} \qquad (8)$$

OPTIMIZATION RESULTS WITH MLI

As an illustration a cryostat with a glass-fibre/epoxy neck and one radiation shield as depicted in Fig. 4 is considered .The emissivity of the container and the outside vessel is 0.1 (e.g. stainless-steel surface) whereas the radiation shield has an emissivity of 0.04 (copper) .Three cases are optimized with respect to the position x of the radiation shield connection on the cryostat neck: no MLI, optimum MLI between vessel and shield and a few layers of MLI. In the first case the optimum position x is 2.7 cm resulting in an evaporation rate of about 3 litres per day. The corresponding heat flows are given in Fig. 5a. The second case of optimum MLI gives 26.9 layers of superinsulation per cm resulting in 67 layers in total. The optimum shield position x is 7.0 cm giving an evaporation rate of 0.5 litre per day (see Fig. 5b). In the third case an MLI blanket of 10 layers with a total thickness of 3 mm is considered. As may be expected from Fig. 3a, this small number of layers already results in a strong reduction of the evaporation rate: 0.8 litre per day with an optimum shield position of 6.6 cm (see Fig. 5c).

CONCLUSION

The CACD programs have been extended with the possible application of multi-layer superinsulation. At present, the programs are used in our glassfibre-cryostat development for biomagnetism and special attention will be paid to the heat-exchange mechanism between helium gas and cryostat neck. If this exchange appears to be not ideal, an adapted exchange-model will be developed.

REFERENCES

1. Ter Brake, H.J.M., Den Breeijen, P.M. and Flokstra, J., Proc. ICEC 11, West-Berlin, West-Germany (1986), pp. 549-555.
2. Leung, E.M.W. et al., Adv. Cryo. Eng., vol. 25 (1979), pp. 489-499.
3. Zhitomirskij, I.S. et al., Cryogenics, vol. 19 (1979), pp. 265-268.
4. Matsuda, A. and Yoshikiyo, H., Cryogenics, vol. 20 (1980), pp. 135-138.
5. Verkin, B.I. et al., Proc. ICEC 10, Helsinki, Finland (1984), pp. 529-538.
6. Maiti, C.R., Ind. J. Pure & Appl. Phys., vol. 19 (1981), pp. 571-573.
7. Giani, S. and Giani, L., Ind. J. Cryogenics, vol. 2 (1977), pp. 151-167.
8. Shu, Q.S. et al., Adv. Cryo. Eng., vol. 31 (1986), pp. 455-463.
9. Shu, Q.S. et al., Cryogenics, vol. 26 (1986), pp. 671-677.
10. Scurlock, R.G. and Saull, B., Cryogenics, vol. 16 (1976), pp. 303-311.
11. Barron, R., Cryogenic Systems, Mc Graw-Hill Book Company, New York (1966).
12. Hnilicka, M.P., Adv. Cryo. Eng., vol. 5 (1960), pp. 199-208.

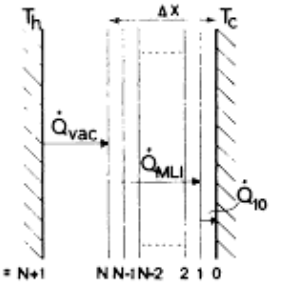

Fig. 1: MLI heat-flow model

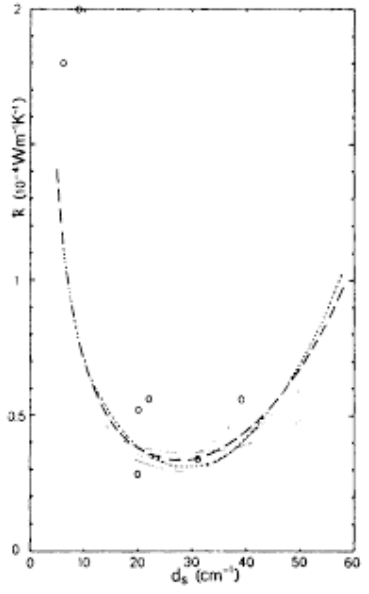

Fig. 2: Mean effective thermal conductivity of an MLI blanket as a function of the layer density (T_h = 300 K, T_c = 77 K):
– – – according to eq.(2)
------ according to Barron [11]
——— calorimetric results presented in [5]
o results presented in [10]

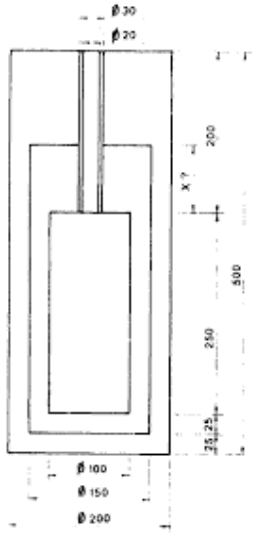

Fig. 4: Dimensions of the cryostat for MLI calculations (in mm)

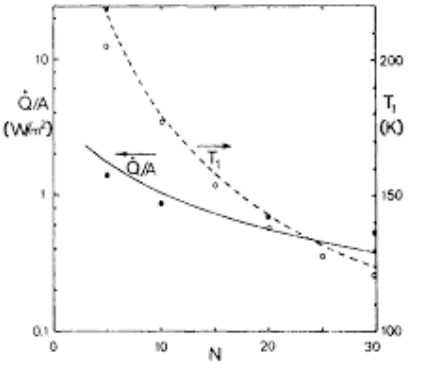

Fig. 3a: Heat flux as a function of the number of MLI layers:
● data presented in [9] for NRC-2
——— heat flux according to the model

3b: Temperature of the first MLI layer as a function of the number of layers:
o data presented in [9] for NRC-2
----- temperature according to the model

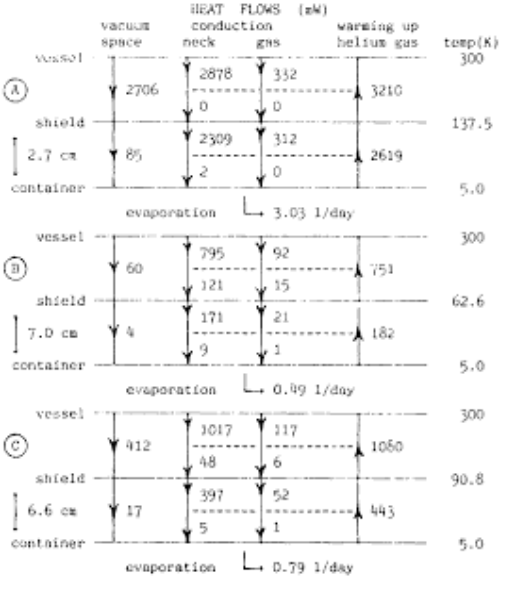

Fig. 5: Heat-flow diagrams for the cryostat of Fig. 4 for three MLI-cases:
A: no MLI
B: optimum MLI (67 layers)
C: 10 layers, thickness 3 mm